Tetrahedron Letters 49 (2008) 5515–5518

Contents lists available at ScienceDirect

Tetrahedron Letters

journal homepage: www.elsevier.com/locate/tetlet

Self-assembly via intermolecular hydrogen-bonding between *o*-/*m*-/*p*-NH_2 and BF_2 groups on dipyrromethenes

Ji-Young Shin, Brian O. Patrick, David Dolphin *

Department of Chemistry, University of British Columbia, 2036 Main Mall, Vancouver, Canada BC V6T 1Z1

ARTICLE INFO

Article history:
Received 4 April 2008
Revised 2 July 2008
Accepted 7 July 2008
Available online 11 July 2008

Keywords:
Boron-dipyrromethene
Hydrogen-bond
Self-assembly

ABSTRACT

Boron difluoride dipyrromethenes bearing configurationally different amine groups on a *meso*-phenyl ring were prepared and crystallized. The *ortho*- and *para*-amino groups allow the phenyl group to inductively release greater electron density into the dipyrromethenes resulting in relatively strong intermolecular hydrogen-bonding with the terminal BF_2 groups, whereas the meta-analog formed weaker hydrogen-bonds. The intensities of the ^1H NMR peaks in concentrated solutions all increased with F-decoupling.

The chemistry of inter- and intramolecular interactions that result in the self-assembly of supramolecules is attracting considerable interest in many diverse areas of chemistry, physics, engineering, and crystal design.[1–8] Within the framework of supramolecular chemistry, dipyrromethene analogs have recently been seen as an interesting group of ligands and several of our studies in related areas have been reported.[9–12] In this Letter, we report the structures of various self-assemblies generated through intermolecular hydrogen-bonding between *o*-, *m*-, or *p*-amines on *meso*-aryl groups and BF_2 chelates of dipyrromethenes. We anticipated that delocalization of an amine lone pair on a *meso*-aryl group would inductively increase electron density into the dipyrromethene and at boron making the fluorine atoms better donors. The near orthogonality of the phenyl and dipyrromethene chromophores suggests that resonance delocalization will be at a minimum and that inductive effects will play a dominant role.

NO_2-substituted aryldipyrromethanes **1**–**3** were prepared from nitrobenzaldehyde and 2-methylpyrrole by general synthetic methods.[13] The NO_2-substituted aryldipyrromethene **4** was prepared from 4′-nitrobiphenyl-4-carbaldehyde and 2-methylpyrrole followed by oxidation with 2,3-dichloro-5,6-dicyano-1,4-benzoquinone. Upon treatment of acetonitrile solutions of each dipyrromethene with triethylamine and boron trifluoro-etherate, compounds **5**–**8** were isolated by column chromatography on silica gel. The title compounds **9**–**12** were obtained by reducing **5**–**8** with hydrazine and palladium carbon. The structures were determined by X-ray diffraction analysis (Scheme 1).[14–17]

The molecules of **9** show two different patterns of hydrogen-bonding (Fig. 1). Pattern A (top of Fig. 1) shows hydrogen-bonding between the two amines and the two boronic fluorides of four neighboring molecules, closely approximating the corners of a square. The lengths of these hydrogen-bonds are 2.098 Å for a and 2.502 Å for b. Pattern B (bottom of Fig. 1) has strong NH–F

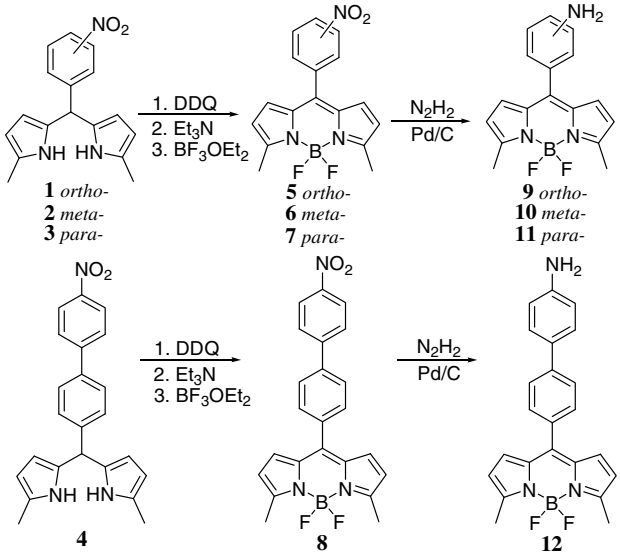

Scheme 1. Synthetic routes for **9**, **10**, **11**, and **12**.

* Corresponding author. Tel.: +1 604 822 3200; fax: +1 604 822 9678.
E-mail address: david.dolphin@ubc.ca (D. Dolphin).

0040-4039/$ - see front matter © 2008 Elsevier Ltd. All rights reserved.
doi:10.1016/j.tetlet.2008.07.045

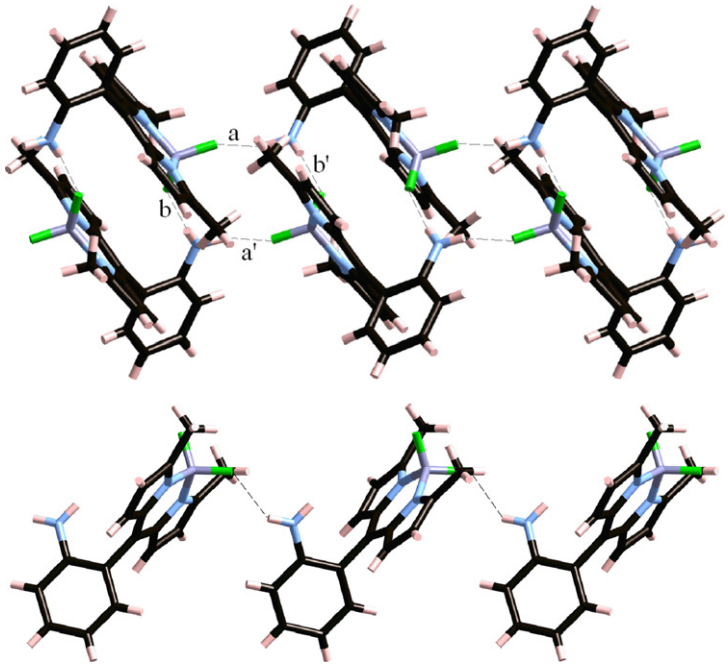

Figure 1. Intermolecular hydrogen-bonding patterns of compound **9** (a = a′, b = b″); pattern A (top) pattern B (bottom).

Table 1
Selected bond angles and distances

Compound	F–H distances (Å)		H–N distances (Å)		F–N distances (Å)		F–H–N angles (°)	
9	F3–H6B	2.15	H6B–N6	0.88	F3–N6	2.90	N6–H6B–F3	142.7
	F1–H3B[1]	2.50	H3B–N3	0.91	F1–N3	3.31	N3–H3B–F1	148.7
	F2–H3A[2]	2.10	H3A–N3	0.88	F2–N3	2.97	N3–H3A–F2	171.6
10	F1–H4[3]	2.44	H4–N3	0.88	F1–N3	3.26	F1–H4–N3	156.1
	F2–H4[4]	2.59			F2B–N3B	3.52	F2–H4–N3	150.5
	F2–H3[5]	2.81	H3–N3	0.90	F2A–N3A	3.39	F2–H3–N3	136.1
11	F4–H3A[6]	2.24	H3A–N3	0.89	F4A–N3	3.02	F4–H3A–N3	180.0
	F4–H3B[7]	2.37	H3B–N3	0.88	F4B–N3	3.10	F4–H3B–N3	132.0
	F1–H6A[8]	2.24	H6A–N6	0.92	F1–N6	2.95	F1–H6A–N6	132.5
12	F1–H2	2.30	H2–N3	0.87	F1–N3	2.90	F1–H2–N3	126.6
	F2–H1	2.49	H1–N3	0.88	F2–N3	3.00	F2–H1–N3	118.3

[1]a and [2]b for the pattern A (top) in Figure 1; [3]c, [4]b and [5]a in Figure 2; [6]b, [7]a, and [8]c in Figure 3.

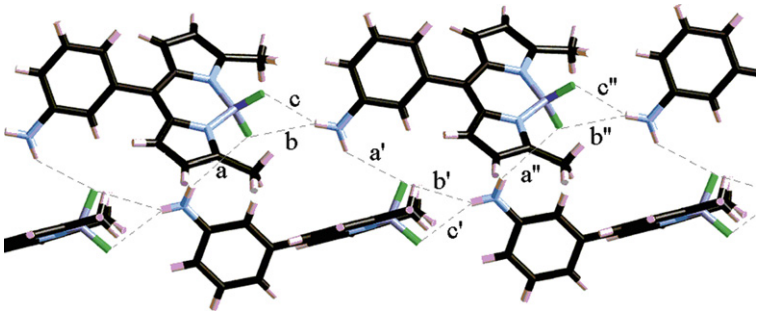

Figure 2. Intermolecular hydrogen-bonding patterns of compound **10** (a = a′ = a″, b = b′ = b″, c = c′ = c″).

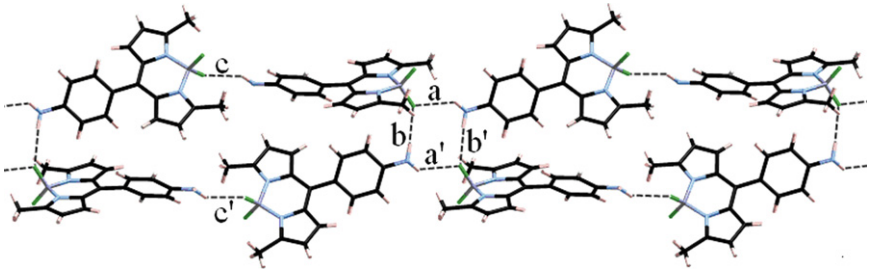

Figure 3. Intermolecular hydrogen-bonding patterns of compound **11** (a = a′, b = b′, c = c′).

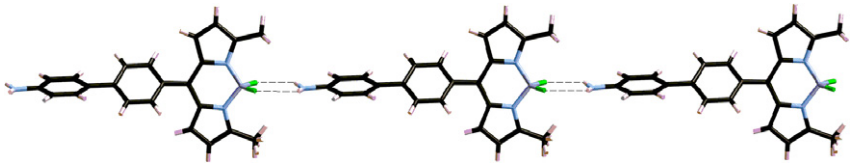

Figure 4. Intermolecular hydrogen-bonding pattern of compound **12**.

hydrogen-bonding using only a single H-atom of the amine and here the hydrogen-bond distance is 2.148 Å. These two different patterns are also found in the crystal structure of **11** (Fig. 3) with hydrogen-bond distances of 2.369 Å, 2.235 Å, and 2.242 Å for a, b, and c, respectively. Delocalization of the *ortho*- and *para*-amino groups into the aromatic systems should result in a similar inductive effect on *meso*-position of the conjugated dipyrromethene moiety and indeed, the two systems show similar hydrogen-bonding motifs and similar bond lengths, Table 1.

On the other hand, the *meta*-amine of **10** (Fig. 2) formed weak NH–F hydrogen-bonds, (Table 1). Compound **12**, containing a biphenyl-amino group, showed hydrogen-bond lengths similar to those in **9** and **11**, where both H atoms on the phenylamines make hydrogen-bonds with one BF_2 chelate of a neighboring molecule (Fig. 4).

Table 1 shows selected bond distances and angles relating to the hydrogen-bonding motifs found in the crystal structures. Since all three structures exhibit different hydrogen-bonding motifs a detailed comparison is not warranted. However, it is clear, as shown by the N–H and F–N distances that compound 10 which contains the *m*-amino group has a relatively weaker hydrogen-bond.

The hydrogen-bonds in solution were confirmed by ^{19}F-decoupled ^{1}H NMR spectroscopy.[18] The differences between ^{19}F-coupled and ^{19}F-decoupled ^{1}H NMR spectra for CD_2Cl_2 solution of **9**–**12** are shown in Figure 5. To maximize intermolecular hydrogen-bonding, highly concentrated solutions were used for the NMR analysis. The highest upfield signals shown in Figure 3a, c, e, and g, based on the ^{19}F-coupled ^{1}H NMR spectra, represent the amino-Hs on the *meso*-aryl groups. The signals appeared at 3.82, 3.87, 4.11, and 3.88 ppm for compounds **9**, **10**, **11**, and **12**, respectively. As shown in Figure 5b, d, f, and h, the amine-H signals increased when ^{19}F-decoupled. While the chemistry of boron dipyrromethene complexes have been widely studied,[19–21] their macromolecular structure is also proving to be an interesting aspect of their chemistry.

The ability to determine hydrogen-bond strength using bond distances is contentious. An intramolecular-inductive effect into dipyrromethene moieties, as a result of resonance delocalization, can influence intermolecular hydrogen-bonding networks. The simple systems described in this Letter have provided an introduction to the generation of self-assemblies using intermolecular hydrogen-bonding within dipyrromethenes. Studies on more complex systems are continuing.

Acknowledgments

This work was supported by the Natural Science and Engineering Research Council (NSERC) of Canada. The authors thank the mass spectroscopy lab of the UBC Department of Chemistry.

Supplementary data

Supplementary data associated with this article can be found, in the online version, at doi:10.1016/j.tetlet.2008.07.045.

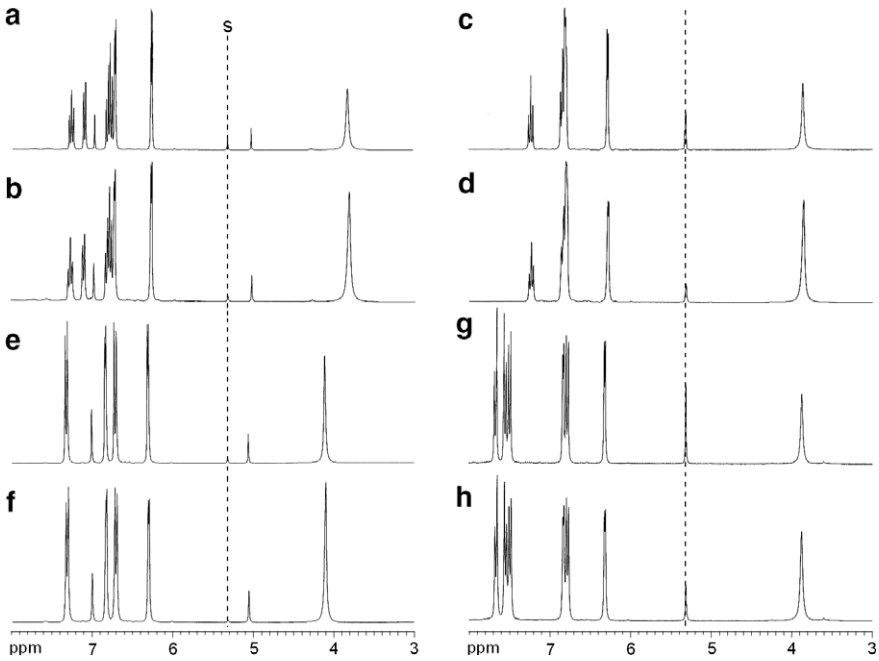

Figure 5. ^{1}H NMR (CD_2Cl_2) spectral changes of the amino group upon ^{19}F-decoupling: before (a, c, e, and g) and after (b, d, f, and h) decoupling of compounds **9**, **10**, **11**, and **12** in. **S** is the solvent peak.

References and notes

1. Desiraju, G. R. *Crystal Engineering: The Design of Organic Solids*; Elsevier: Amsterdam, 1989.
2. Lehn, J.-M. *Supramolecular Chemistry: Concepts and Perspectives*; VCH: Weinheim, 1995.
3. *Comprehensive Supramolecular Chemistry*; Atwood, J. L., Davies, J. E. D., MacNicol, D. D., Vögtle, F., Lehn, J.-M., Eds.; Pergamon: Oxford, 1996.
4. Desiraju, G. R. *Nature* **2001**, *412*, 397.
5. Hollingsworth, M. D. *Science* **2002**, *295*, 2410.
6. MacDonald, J. C.; Dorrestein, P. C.; Pilley, M. M.; Foote, M. M.; Lundburg, J. L.; Henning, R. W.; Schultz, A. J.; Manson, J. L. *J. Am. Chem. Soc.* **2000**, *122*, 11692.
7. Moulton, B.; Zaworotko, M. J. *Chem. Rev.* **2001**, *101*, 1629.
8. Sommerdijk, N. A. J. M. *Angew. Chem., Int. Ed.* **2003**, *42*, 3572.
9. Chen, Q.; Dolphin, D. *Can. J. Chem.* **2002**, *80*, 1668.
10. Thompson, A.; Rettig, S. J.; Dolphin, D. *Chem. Commun.* **1999**, 631.
11. Zhang, Y.; Thompson, A.; Rettig, S. J.; Dolphin, D. *J. Am. Chem. Soc.* **1998**, *120*, 13537.
12. Shin, J.-Y.; Dolphin, D.; Patrick, B. O. *Cryst. Growth Des.* **2004**, *4*, 659.
13. Wagner, R. W.; Lindsey, J. S. *Pure Appl. Chem.* **1996**, *68*, 1373.
14. Analytical data for compound **9** (mp = 167–169 °C) ^{1}H NMR at rt ($CDCl_3$, 300 MHz) δ = 7.54 (t, J = 8.3, 1H), 7.38 (dd, J = 7.6, ^{dd}J = 1.4, 1H), 7.10 (t, J = 7.5, 1H), 7.04 (d, J = 8.2, 1H), 7.00 (d, J = 4.0, 2H), 6.52 (d, J = 4.1, 2H), 3.07 (br s, 2H), 2.93 (s, 6H); ^{13}C NMR at rt (CD_2Cl_2, 100.64 MHz) δ = 158.52, 145.30, 140.48, 135.06, 131.83 (CH), 131.11 (CH), 130.52 (CH, 2C), 120.05 (CH, 2C), 119.33, 118.08 (CH), 116.48 (CH), 15.23 (CH_3, 2C); EIMS m/z ($C_{17}H_{16}{}^{11}BF_2N_3$, m/z) found 311.14156, calcd 311.14053; UV–vis (CH_2Cl_2) λ_{max}/nm (log ε) 333 (4.00), 515 (4.95). Crystal data for **9**: $C_{17}H_{16}N_3F_2B$, T = 173 K, M_w = 311.14, monoclinic, $P2_1/c$(#14), a = 21.3685(13) Å, b = 9.6969(4) Å, c = 16.0314(9) Å, β = 110.662(3)°, V = 3108.2(3) Å^3, D_c = 1.330 g cm^{-3}, Z = 8, $R1$ = 0.0494 ($I > 2.00\sigma(I)$), $wR2$ = 0.141 (all data), GOF = 1.02. CCDC 683839.
15. Analytical data for compound **10** (mp = 225–227 °C) ^{1}H NMR at rt (CD_2Cl_2, 300 MHz) δ = 7.32 (t, J = 7.7, 1H), 6.75–6.91 (m, 4H), 6.82 (s, 1H), 6.29 (d, J = 4.1, 2H), 3.87, (br s, 2H), 2.60 (s, 6H); ^{13}C NMR at rt (acetone-d_6, 100.64 MHz) δ = 157.99, 149.50, 135.61, 135.23, 131.43 (CH, 2C), 129.89 (CH), 120.16 (CH), 120.13 (CH, 2C), 119.95 (CH), 116.98 (CH), 14.94 (CH_3, 2C); ESIMS 334.2 m/z ([M+Na]$^+$); elemental analysis ($C_{17}H_{16}{}^{11}BF_2N_3$, %) found 13.66 (N), 65.85 (C), 5.50 (H), calcd 13.51 (N), 65.62 (C), 5.18 (H); UV–vis (CH_2Cl_2) λ_{max}/nm (log ε) 338 (4.20), 512 (5.07). Crystal data for **10**: $C_{17}H_{16}N_3F_2B$, T = 173 K, M_w = 311.14, monoclinic, $P2_1/n$(#14), a = 7.4989(3) Å, b = 20.5912(8) Å, c = 9.7926(3) Å, β = 98.401(1)°, V = 1495.86(10) Å^3, D_c = 1.382 g cm^{-3}, Z = 4, $R1$ = 0.0402 ($I > 2.00\sigma(I)$), $wR2$ = 0.112 (all data), GOF = 1.06. CCDC 683840.
16. Analytical data for compound **11** (mp = 155–167 °C) ^{1}H NMR at rt (CD_2Cl_2, 300 MHz) δ = 7.23 (t, J = 7.7, 1H), 6.85 (d, J = 7.7, 2H), 6.81 (d, J = 3.7, 2H), 6.79 (s, 1H), 6.29 (d, J = 4.0, 2H), 3.87 (s, 2H), 2.60 (s, 6H); ^{13}C NMR at rt (acetone-d_6, 100.64 MHz) δ = 156.32, 134.98, 133.53, 130.94, 122.90, 119.58, 114.62, 120.48, 14.85; ESIMS 334.2 m/z ([M+Na]$^+$); UV–vis (CH_2Cl_2) λ_{max}/nm (log ε) 437 (4.04), 482 (4.31), 508 (4.84). Crystal data for **11**: $C_{17}H_{16}N_3F_2B$, T = 173 K, M_w = 311.14, monoclinic, $P2_1/n$(#14), a = 9.8037(5) Å, b = 23.8594(11) Å, c = 13.3120(6) Å, β = 103.055(2)°, V = 3033.3(2) Å^3, D_c = 1.363 g cm^{-3}, Z = 8, $R1$ = 0.0447 ($I > 2.00\sigma(I)$), $wR2$ = 0.118 (all data), GOF = 1.03. CCDC 683841.
17. Analytical data for compound **12** (mp = >230 °C) ^{1}H NMR at rt (CD_2Cl_2, 300 MHz) δ = 7.67 (d, J = 8.3, 2H), 7.55 (d, J = 8.3, 2H), 7.49 (d, J = 8.5, 2H), 6.83 (d, J = 3.9, 2H), 6.78 (d, J = 8.5, 2H), 6.32 (d, J = 3.9, 2H), 3.88 (br s, 2H), 2.62 (s, 6H); ^{13}C NMR at rt (acetone-d_6, 100.64 MHz) δ = 158.26, 157.97, 149.86, 144.35, 143.57, 135.11, 133.31, 132.20, 132.10 (CH, 2C), 131.32 (CH, 2C), 128.65 (CH, 2C), 126.40 (CH, 2C), 120.38 (CH, 2C), 115.68 (CH, 2C), 14.95 (CH_3, 2C); ESIMS 410.3 m/z ([M+Na]$^+$); elemental analysis ($C_{23}H_{20}{}^{11}BF_2N_3$, %) found 10.58 (N), 71.10 (C), 5.60 (H), calcd 10.85 (N), 71.34 (C), 5.21 (H); UV–vis (CH_2Cl_2) λ_{max}/nm (log ε) 415 (4.54), 512 (5.34). Crystal data for **12**: $C_{23}H_{20}N_3F_2B$, T = 173 K, M_w = 387.23, monoclinic, $P2_1/c$(#14), a = 11.3809(14) Å, b = 13.251(2) Å, c = 12.5306(14) Å, β = 92.778(4)°, V = 1887.5(4) Å^3, D_c = 1.363 g cm^{-3}, Z = 4, $R1$ = 0.0431 ($I > 2.00\sigma(I)$), $wR2$ = 0.109 (all data), GOF = 1.02. CCDC 683842.
18. Gossauer, A.; Fehr, F.; Nydegger, F.; Stöckli-Evans, H. *J. Am. Chem. Soc.* **1997**, *119*, 1599.
19. Pagano, R. E.; Martin, O. C.; Kang, H. C.; Haugland, R. P. *J. Cell. Biol.* **1991**, *113*, 1267.
20. Bricks, J. L.; Kovalchuk, A.; Trieflinger, C.; Nofz, M.; Büschel, M.; Tolmachev, A. I.; Daub, J.; Rurack, K. *J. Am. Chem. Soc.* **2005**, *127*, 13522.
21. Costela, A.; García-Moreno, I.; Cómez, C.; Amat-Guerri, F.; Liras, M.; Sastre, R. *Appl. Phys. B* **2003**, *76*, 365.